

## CRITICAL REVIEW

# PTCOG Ocular Statement: Expert Summary of Current Practices and Future Developments in Ocular Proton Therapy

Jan Hrbacek, PhD,\* Andrzej Kacperek, PhD,<sup>†</sup> Jan-Willem M. Beenakker, PhD,<sup>‡,§,||,¶</sup> Linda Mortimer, PhD,<sup>#</sup> Andrea Denker, PhD,\*\* Alejandro Mazal, PhD,<sup>††</sup> Helen A. Shih, MD, MS, MPH, FASTRO,<sup>‡‡,§§</sup> Remi Dendale, MD,<sup>||</sup> Roelf Slopsema, MS,<sup>¶¶</sup> Jens Heufelder, PhD,<sup>##,2</sup> and Kavita K. Mishra, MD MPH<sup>\*\*\*,2</sup>

\*Center for Proton Therapy, Paul Scherrer Institute, Villigen, Switzerland; <sup>†</sup>University College London, London, United Kingdom; <sup>‡</sup>Department of Ophthalmology, Leiden University Medical Center, Leiden, Netherlands; <sup>§</sup>Department of Radiology, C.J. Gorter MRI Center, Leiden University Medical Center, Leiden, Netherlands; <sup>||</sup>Department of Radiation Oncology, Leiden University Medical Center, Leiden, Netherlands; <sup>¶</sup>HollandPTC, Delft, Netherlands; <sup>#</sup>Medical Physics Department, The Clatterbridge Cancer Centre NHS Foundation Trust, Birkenhead, United Kingdom; <sup>\*\*</sup>Helmholtz-Zentrum Berlin für Materialien und Energie, Proton Therapy (BE-APT), Berlin, Germany; <sup>††</sup>Medical Physics Service, Centro de Protonterapia Quironsalud, Madrid, Spain; <sup>‡‡</sup>Harvard Medical School, Boston, Massachusetts; <sup>§§</sup>Department of Radiation Oncology, Massachusetts General Hospital, Boston, Massachusetts; <sup>||</sup>Institut Curie Protontherapy Center, Orsay, France; <sup>¶¶</sup>Department of Radiation Oncology, Emory Proton Therapy Center, Atlanta, Georgia; <sup>##</sup>Department of Ophthalmology, Charité – Universitätsmedizin Berlin, Berlin/Protonen am HZB, Berlin, Germany; and <sup>\*\*\*</sup>Proton Ocular Radiation Therapy Program, Department of Radiation Oncology, Osher Center for Integrative Health, Osher Foundation Endowed Chair in Clinical Programs in Integrative Health, University of California San Francisco, San Francisco, California

Received Jul 13, 2023; Accepted for publication Jun 18, 2024

## Abstract

Although rare cancers, ocular tumors are a threat to vision, quality of life, and potentially life expectancy of a patient. Ocular proton therapy (OPT) is a powerful tool for successfully treating this disease. The Particle Therapy Co-Operative Ocular Group) formulated an Evidence and Expert-Based Executive Summary of Current Practices and Future Developments in OPT: comparative dosimetric and clinical analysis with the different OPT systems is essential to set up planning guidelines, implement best practices, and establish benchmarks for eye preservation, vision, and quality of life measures. Contemporary prospective trials in select subsets of patients (eg, tumors near

Corresponding author: Jan Hrbacek, PhD; E-mail: [jan.hrbacek@psi.ch](mailto:jan.hrbacek@psi.ch)

Disclosures: J.H. is consultant of Med Austron and Westdeutsches Protontherapiezentrum. J.W.M.B. receives research support from Philips Healthcare and RaySearch Laboratories, also receives grant support from HollandPTC and Varian Medical Systems, and as well as other support from Philips Healthcare and RaySearch Laboratories. A.M. is consultant and has received honoraria from Ion Beam Applications, and is also a member of the PTCOG committee. H.A.S. is consultant of Ion Beam Application. The other authors have no conflicts of interest to declare.

Data Sharing Statement: Given the nature of the presented manuscript, which is an expert critical review, a formal data sharing statement may not be applicable. Because the manuscript primarily involves a comprehensive analysis and evaluation of existing literature and expert opinions, it may not involve specific data sets or raw data that can be shared. However, the findings, conclusions, and references mentioned in the manuscript can serve as a valuable resource for further research and discussion in the field.

*Acknowledgments*—The authors would like to express their gratitude to the contributors of the symposium, whose presentations and insights have been instrumental in the creation of this state-of-the-field manuscript: Nathalie Cassoux (France), Mario Ciocca (Italy), Inder Daftari (United States), Roi Dagan (United States), Bertil Damato (United Kingdom), Amanda Deisher (United States), Lia Halasz (United States), William Hartsell (United States), Heinrich Heimann (United Kingdom), Joël Héroult (France), Antonia Jousen (Germany), Nobuyuki Kanematsu (Japan), Rashmi Kapur (United States), Benjamin Koska (Germany), Jon Kruse (United States), Maria Mamalui (United States), Catherine Nauraye (France), Alessia Pica (Switzerland), Ann Schalenbourg (Switzerland), Jessica Scholey (United States), Kees Spruijt (Netherlands), Jan Swakon (Poland), Juliette Thariat (France), Alexei Trofimov (United States), Berit Verbist (Netherlands), Riccardo Via (Switzerland), and Jörg Wulf (Germany).

<sup>2</sup> Jens Heufelder and Kavita K. Mishra shared the last authorship.

the optic disc and/or macula) may allow for dosimetric and clinical analysis between different radiation modalities and beamline systems to evaluate differences in radiation delivery and penumbra, and resultant tumor control, normal tissue complication rates, and overall clinical cost-effectiveness. To date, the combination of multimodal imaging (fundus photography, ultrasound, etc), ophthalmologist assessment, and clip surgery with radiation planning have been keys to successful treatment. Increased use of three-dimensional imaging (computed tomography/magnetic resonance imaging) is anticipated although its spatial resolution might be a limiting factor (eg, detection of flat diffuse tumor parts). Commercially produced ocular treatment-planning systems are under development and their future use is expected to expand across OPT centers. Future continuity of OPT will depend on the following: (1) maintaining and upgrading existing older dedicated low-energy facilities, (2) maintaining shared, degraded beamlines at large proton therapy centers, and (3) developing adapted gantry beams of sufficient quality to maintain the clinical benefits of sharp beam conformity. Option (1) potentially offers the sharpest beams, minimizing impact on healthy tissues, whereas (2) and (3) potentially offer the advantage of substantial long-term technical support and development as well as the introduction of new approaches. Significant patient throughputs and close cooperation between medical physics, ophthalmology, and radiation therapy, underpinned by mutual understanding, is crucial for a successful OPT service. © 2024 The Author(s). Published by Elsevier Inc. This is an open access article under the CC BY license (<http://creativecommons.org/licenses/by/4.0/>)

## Introduction

Ocular tumors are rare cancers that can threaten vision, quality of life, and potentially life expectancy. Overall, proton radiation therapy (RT) is associated with excellent local tumor control and eye preservation rates for malignant and benign ocular conditions.

The Particle Therapy Co-Operative Ocular Group (PTCOG Ocular) is the international consortium of proton and particle beam therapy institutions treating patients with ocular tumors.<sup>1</sup> Given the rarity of this ocular disease and the significant growth of proton centers over the past decade, clinical practice statements derived from the evidence and expert consensus are particularly critical to ensure high quality and appropriate care. The current report highlights the current practice and results of the second global multi-institutional survey, as detailed at the inaugural PTCOG International Ocular Proton Therapy Symposium.<sup>2,3</sup>

Summarizing the current state and areas of future development in proton ocular treatment provides the necessary benchmarks to maintain patient-centered care and maximize local control, vision, and quality of life. This executive summary of established literature, complemented with expert opinion and selected survey results, sets the groundwork for assessing subtle and significant variation in practices now and in the future. Ultimately, the goal of the research and development in the ocular community with established and new beamlines is to focus on the patient outcomes and experience, to ensure an appropriate and high standard of excellence in care.

## Clinical Indications for Ocular Proton Therapy

Proton therapy is a well-established and accepted modality for the treatment of uveal melanoma (UM) and other ocular

tumors, as supported by a large body of peer-reviewed literature.<sup>4-21</sup> In total, approximately 47,000 ocular patients have been treated with particle beams worldwide (since 1975) for UM, conjunctival tumors, choroidal metastases, hemangiomas, other vascular tumors, macular degeneration, and retinoblastomas, as primary, salvage, or adjuvant treatment with combined modality therapy.

Studies show UM tumor local control to be approximately 96% at 5 years and maintained at 10 and 15-year follow-up.<sup>4,14-16,19,22,23</sup> Eye preservation rates are approximately 90% at 5 years.<sup>15-19,24,25</sup> Importantly, depending on tumor dimensions and distance to the optic disc and macula, as well as the proton beam penumbra, vision preservation is achievable in specific cases through careful planning of gaze angles, margin selection, and postirradiation ophthalmic interventions. Metastatic disease remains an issue for high-risk patients, with immunotherapy options and continued therapeutic target study on the horizon.<sup>26-28</sup> Recurrences are rare after ocular proton therapy (OPT) and may be due to a marginal or geographic miss or in-field failure for potential radioresistant tumors.<sup>23,29,30</sup> A second course of OPT has been shown to provide acceptable local control and eye preservation.<sup>22,23,29,30</sup>

## Target Volume Definition: Imaging and Surgical Best Practices

Target volume definition for OPT generally includes a combined clinical evaluation with ophthalmic imaging techniques (Fig. 1a, b, g) complemented with surgical placement of tantalum markers at the tumor border. More recently, three-dimensional (3D) radiologic imaging, in particular magnetic resonance imaging (MRI; Figs. 1c and 2),<sup>31</sup> has been introduced in OPT planning as a complementary source of information.

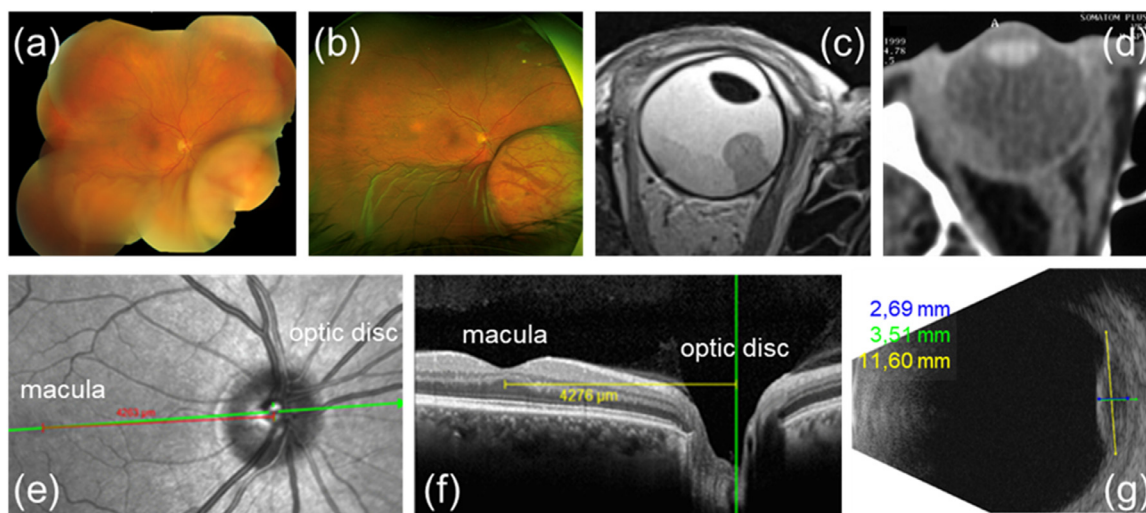


**Fig. 1.** Different imaging modalities in OPT: fundus composite (a), wide-angle fundus (b), transversal MRI slice (c) of the same tumor; transversal CT slice of a different eye with tumor (d), infrared fundus showing macula and optic disc (e). The green line indicates the direction of the OCT slice through the macula and optic disc to determine their distance (f). Ultrasound image of tumor (g) with measurements of height (ex-/including sclera: blue/green line) and base width (yellow line). *Abbreviations:* CT = computed tomography; MRI = magnetic resonance imaging; OCT = ocular coherence tomography; OPT = ocular proton therapy.

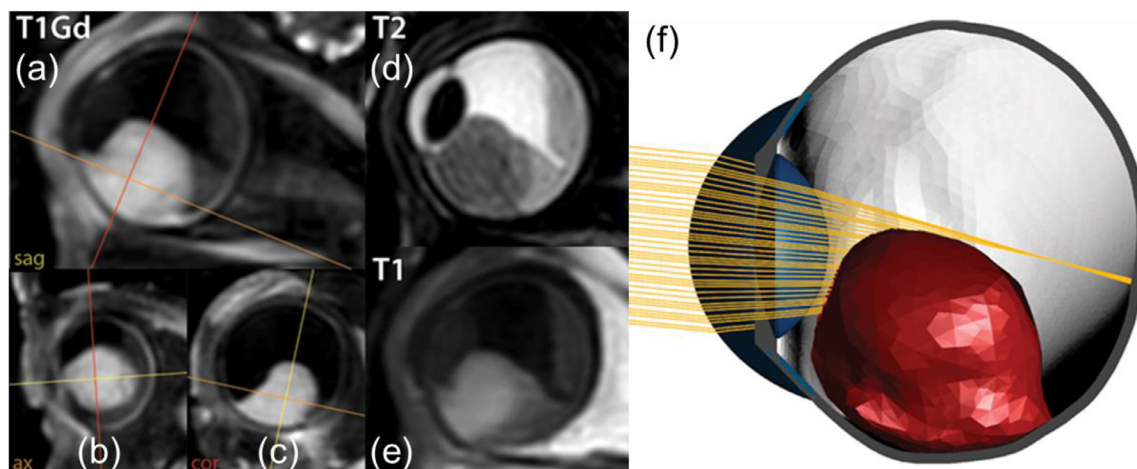


**Fig. 2.** MR-images and ray-tracing model of an eye with an uveal melanoma: 3D T1 weighted contrast enhanced weighted images in the sagittal (a), transversal (b), and coronal (c) plane showing the 3D morphology and location of the tumor; corresponding sagittal slices on T2 (d) and T1 (e) weighted images without contrast enhancement; optical ray-tracing simulation of the same patient (f), showing how the incoming light rays (yellow) are blocked by the tumor.<sup>31</sup> Thus, a shadow (black) is created by the tumor on the retina. *Abbreviations:* 3D = three-dimensional; MR = magnetic resonance.

## Ophthalmic imaging

As part of the standard of care clinical assessment, fundus imaging (FI) is one of the main tools for diagnosis and target delineation in OPT. There are different systems available ranging from composite images consisting of relatively small images to 200-degree ultra-wide-angle false color systems. All these systems can be used in OPT to provide indirect information about the shape of the tumor and its location in relation to other anatomic structures (Fig. 1a, b),<sup>32-34</sup> but if

they are to be used for geometrically accurate tumor delineation, their registration on the eye model must take into account the characteristics of the camera used. One limitation of FI is in prominent lateral or anterior tumors, where the posterior part of the tumor base is occluded by the tumor apex (Figs. 1a-c and 2d, e).<sup>35,36</sup> Another limitation is the optical distortion of FI, which can lead to geometric discrepancies due to a simple 2-point registration typically used in treatment-planning systems (TPS; Fig. 3c). A more sophisticated method, based on registration of FI with a

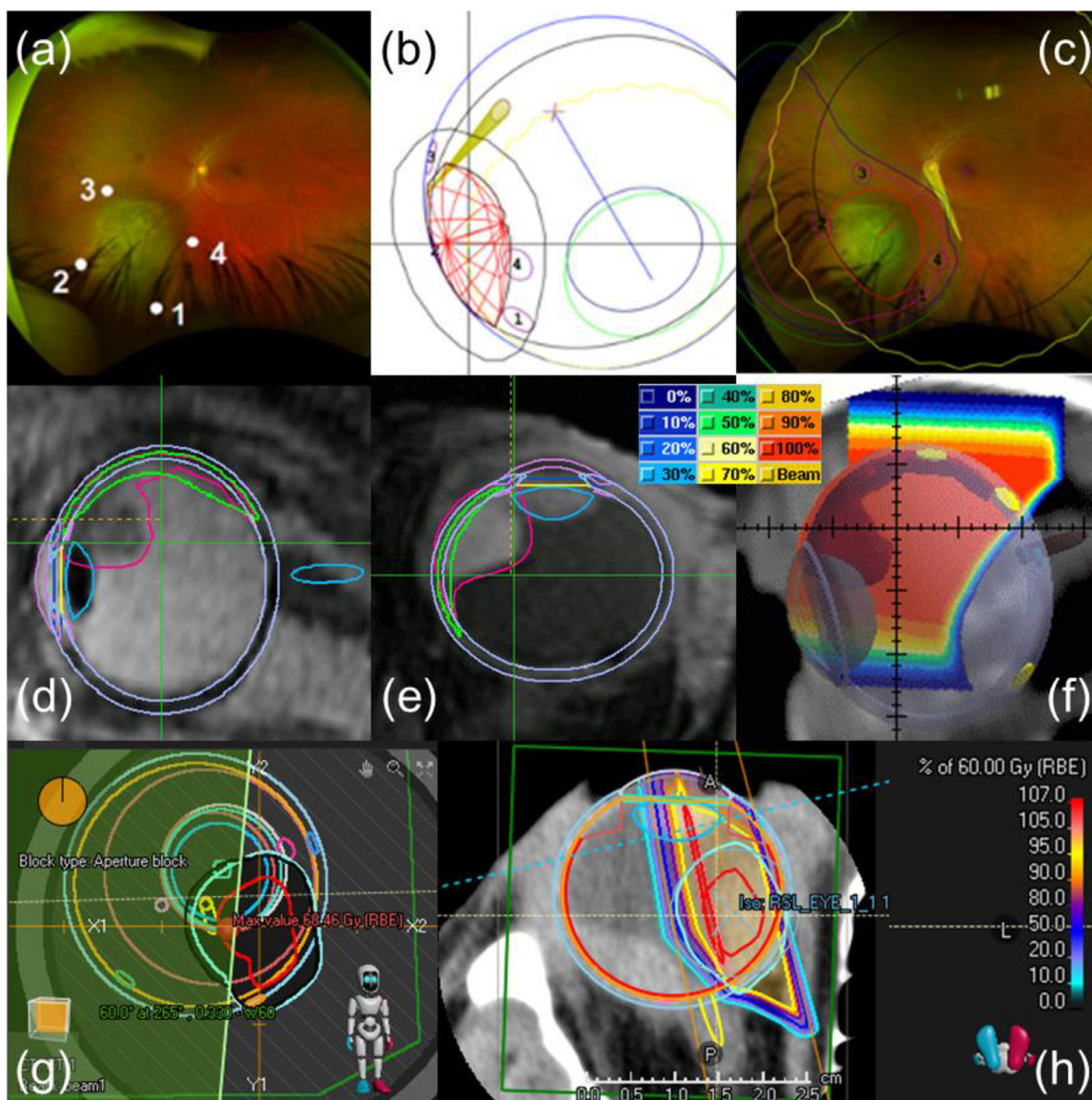


**Fig. 3.** Treatment planning in EYEPLAN (top row): fundus photograph clip assessment by the ophthalmologist (a); beams-eye-view (b) of treatment plan showing eye model with tumor (red), clip positions (1-4) and collimator outline (black); corresponding dose distribution (shown isodoses: 90%—dark red, 50%—blue, and 10%—green) on the coregistered fundus (c) — the tumor base is surrounded by the 4 tantalum clips (1-4) and marked as clinical target volume (red). OCTOPUS (middle row): Sagittal T2 weighted MRI slice with fundus based contour for marking flat tumor extensions not visible in MRI (green) and MRI-based contour (red; d); transversal T1 weighted MRI slice with both contour sets (red, green; e); lateral view of 3D eye model with dose distribution on CT slice (f). For this anterior ciliary body melanoma, the sharp distal fall-off allows dose sparing of the posterior risk structures: macula, optic disc, and nerve (f). RayOcular (bottom row): Beams-eye-view of treatment plan with wedge (g) and transversal CT-slice with isodose and corresponding color map (h). The wedge reduces the dose to optic disc, nerve, and macula (h). The integrated pencil beam algorithm models the additional lateral scattering of the protons introduced by the wedge on the left part of the treatment field (h). *Abbreviations:* 3D = three-dimensional; CT = computed tomography; MRI = magnetic resonance imaging.

digitally reconstructed fundus from MRI, has been recently described by Via et al.<sup>37</sup>

Other optical-based imaging techniques such as fundus autofluorescence, fluorescein angiography, and indocyanine green angiography are primarily used as differential diagnostic tools to distinguish between choroidal nevus, melanoma,

hemangioma, or metastasis.<sup>34,38,39</sup> In addition, ocular coherence tomography can be used in diagnosis<sup>34,40</sup> and to provide the macular position with respect to the optic disc (Fig. 1e, f), helping to register the FI to the eye model.<sup>41,42</sup> For posterior-located tumors, one can measure the distance between the tumor margin and optic disc and/or macula with high precision.

Ultrasound is often decisive for the diagnosis of small melanomas, showing an increase in the size of the tumor on 2 successive examinations. It is the standard tool for characterizing the dimensions of the tumor, eg, base, height (Fig. 1g), and the distance to optic disc (Table 1). For many OPT centers, ultrasound measurements, FI, and intraoperative caliper measurements represent the primary data elements for treatment planning.<sup>43</sup>

## Tantalum marker placement and planning target volume definition

Tantalum marker (clips) ocular surgery and caliper measurements provide crucial information to the treatment planning in OPT (Table 1) and image-guided treatment delivery.<sup>43</sup> Surgical/clinical assessment for OPT can include fundus or iris drawing with markers/tumor, intraoperative photograph of markers, interclip and measurements to limbus/tumor, tumor distances to disc/macula, tumor base/height, clock hours of tumor extension, and eye axial length. Surgical marker-to-limbus, marker-to-marker, and marker-to-tumor measurements are recorded for the purpose of planning.

Additional surgical communication can assist in treatment optimization, including potential areas of extension, diffuse flat or extraocular spread, variable pigmentation causing difficulty with transillumination (eg, nevus of Ota and ocular melanocytosis), intraoperative procedures or

complications (eg, silicone oil tamponade,<sup>44</sup> vitreous hemorrhage, and exudative retinal detachment). These factors may affect treatment planning, tumor delineation, distal and lateral margins, critical structure analysis, gaze angle options, etc. The experience of the ophthalmologist is essential for precise and optimal clip placement, for localizing the tumor boundaries and avoiding potential surgical pitfalls.

Clips play a key role in patient positioning and appropriate planning target volume margin with an advantage when placed in the vicinity of a tumor, allowing for submillimeter alignment of a target with respect to the beam. Typical planning target volume margins are 2 to 3 mm. Complete obviation of fiducial clips, ie, clipless treatment, would mean a significant improvement in patient comfort, reduce the cost of treatment, and eliminate potential risks associated with the surgery. Clinically, tantalum marker surgery may not be advised for a limited cohort of OPT patients due to comorbidities, extremely thin sclera, or rarely by patient preference. In these instances, clinical alignment with landmarks and a “light field” replicating the radiation beam entrance field is used, eg, for iris and small ciliary body melanomas with visible anterior chamber extension.<sup>45</sup> Larger margins (eg, an additional 1 mm circumferentially) for set-up uncertainty can be added at the treatment team’s discretion. Some centers have already adopted clipless treatment for specific anterior tumors, eg, treatment of iris melanoma using a light field or a beam’s eye view camera for positioning.<sup>45-47</sup> The clipless treatment of posterior intraocular tumors is more challenging

**Table 1 Overview of possible intraocular measurements using different modalities**

Parameter/modality	Clip surgery	Biometry	Ultrasound	Fundus	OCT	CT	MRI
Eye length		X				X	X
Eye width						X	X
Limbus diameter	X	X					
Cornea radius		X					
Lens thickness/width		(X)				X	X
Lens position		X				X	X
Macula position				(X)	X		
Tumor thickness			X			(X)	X
Tumor base			X	X		(X)	X
Tumor position				X	(X)	(X)	X
Distance: tumor to clip	X		X			(X)	X
Distance: tumor to optic disc			X		X	(X)	X
Distance: tumor to macula				(X)	X		
Distance: clip to optic disc	(X)		X				X
Distance: macula to optic disc				(X)	X		
Distance: limbus to clip	X						

Possible measurements are marked with X. The usage of modalities marked with (X) is limited and depends on the individual case or measuring device. Reasons for the limitations could be clip artifacts in CT, retinal detachment, or mechanical limitations for measurements during clip surgery (eg, tiny orbit).

*Abbreviations:* CT = computed tomography; MRI = magnetic resonance imaging; OCT = ocular coherence tomography.

as the submillimeter accuracy provided by the clips is not easily achieved. Although substantial effort has been invested to develop a noninvasive system for eye localization, based on video surveillance of the anterior segment,<sup>48-50</sup> the x-ray imaging of clips remains the most accurate and reliable positioning method. Iris pattern morphology analysis is a promising approach to assess eye torsion noninvasively.<sup>51</sup>

### Three-dimensional imaging

The role of 3D imaging in treatment planning for OPT is increasing. Some TPS such as OCTOPUS<sup>52,53</sup> or the RayOcular module from RayStation (RaySearch Laboratories)<sup>41</sup> allow the use of computed tomography (CT) and/or MRI for eye modeling or definition of the clinical target volume.

CT provides geometric information about the eye, the tumor (Fig. 1d) and, when performed after clip surgery, the position of the clips. This information can be used to set up or improve a geometric eye model<sup>43,54</sup> or fit the eye model to the CT scan.<sup>42,52</sup> Additionally, CT can be used to assess the dosimetric effect of a silicone oil or gas tamponade on the proton dose distribution.<sup>55</sup>

Three-Tesla MRI in combination with a surface coil is recommended for imaging the eye,<sup>56-58</sup> as it offers the resolution needed to visualize small invasions of the tumor into adjacent structures, such as the optic nerve.<sup>35,57</sup> Volumetric sequences with submillimeter resolution provide a 3D visualization of the tumor, surrounding tissues, and the clips.<sup>35,56,59,60</sup> This allows a comparison of MR-based and conventional ophthalmic measurements used for OPT planning.<sup>60,61</sup> However, as longer scanning times may result in eye-motion-related artifacts,<sup>56</sup> a high-spatial resolution alone is insufficient to define the tumor extent.

With the advent of more dedicated MRI techniques for diagnosis,<sup>35,56-58,62</sup> treatment planning,<sup>37,60,61,63</sup> and follow-up,<sup>64,65</sup> the optimal MRI protocol depends on the indication.<sup>66</sup> Although for differential diagnosis, Diffusion and Perfusion Weighted Imaging are of great value,<sup>35,57,58,67</sup> for most OPT planning purposes, 3D T1-weighted images after contrast are preferred, because they provide the best discrimination between tumor and retinal detachment (Fig. 2a-c).<sup>35,60</sup> Gradient-echo sequences can aid in clip localization, but are not suitable for accurate measurements due to susceptibility artifacts.<sup>60,68</sup> Generally, MRI and ultrasound dimension measurements match.<sup>63</sup> In a majority of cases, the MRI and intraoperatively determined clip-tumor measurements were in satisfactory agreement.<sup>60</sup> Flat tumor components, however (Fig. 3d, e), can be difficult to delineate on MRI and inclusion of intraoperative assessments and FI is advised.<sup>34,60</sup> MRI may be particularly valuable for anterior tumors, as in these cases, ultrasound can provide inaccurate measurements and the tumor extent may be overestimated intraoperatively (Fig. 2f).<sup>31,60</sup> For mushroom-shaped tumors, MRI provides a valuable 3D representation in contrast to the conventional 1D measurements. In this context, MRI-based OPT planning shows promise.<sup>56,61,69,70</sup>

### Treatment Planning

Because of the small size of the eye, its nearly homogeneous tissue composition and its movability, a dedicated TPS called EYEPLAN was designed in the 1980s.<sup>71</sup> Based on eye length and limbus diameter, a geometric (spherical or ellipsoid) eye model is created and fitted to the clip positions. The positions are derived from orthogonal x-ray imaging. The tumor is defined by drawing a base contour in the fundus or iris plane and by defining the tumor apex, from which a 3D volume is constructed. Modern versions of EYEPLAN (Fig. 3) allow the coregistration of a FI with the eye model,<sup>72</sup> whereas information from other imaging modalities, including CT or MRI, can only be indirectly incorporated.<sup>54,73</sup> EYEPLAN uses a ray-tracing model to calculate the dose distributions and dose-volume histograms.

OCTOPUS, developed by the German Cancer Research Center (DKFZ) in collaboration with the Helmholtz-Zentrum Berlin (HZB) and the Charité – Universitätsmedizin Berlin,<sup>52</sup> was the first TPS allowing the full incorporation of 3D imaging. Although preserving the conventional EYEPLAN approach, a predefined elliptical eye model can be matched to CT/MRI. For dose calculation, a fast ray-tracing algorithm is used.<sup>53</sup> XXX achieves the same tumor control as plans from EYEPLAN.<sup>23</sup> The image-based planning approach requires more time, although the derived eye models appear to be more realistic in certain patients.<sup>42</sup>

More than 90% of the OPT patients to date (~42,000 cases) have been planned with EYEPLAN. Two centers use its commercial equivalent Eclipse Ocular Proton Planning (EOPP, Varian Medical Systems).<sup>14,23,74,75</sup> Additionally, >3500 patients have been planned with OCTOPUS. Further development of EYEPLAN, EOPP, and OCTOPUS has been discontinued.

In 2021, the RayOcular module from RayStation became clinically available and integrates features of EYEPLAN and OCTOPUS into a modern treatment-planning environment (Fig. 3g, h). For dose calculation a pencil beam algorithm is used,<sup>41,76</sup> resulting in more accurate dose distributions.<sup>77</sup>

Although the majority of OPT patients have been treated with beamlines specifically developed for eye treatments, gantry-based or scanning-based OPT systems are also being used. These systems rely on commercially available TPS.<sup>78-80</sup> This allows CT/MRI-based planning, but they cannot use the advantage of coregistered FI for tumor delineation. All ophthalmologic 2D imaging data have to be translated manually for tumor contouring,<sup>79</sup> making OPT planning difficult.

### Critical structure dose optimization/planning best practices

The planning process for OPT prioritizes tumor coverage and normal tissue dose optimization. The dose distribution is calculated with a simple ray-tracing algorithm<sup>71</sup> and can be displayed on the fundus (Fig. 3c), in arbitrary planes, or in risk structure related dose-volume histograms. The

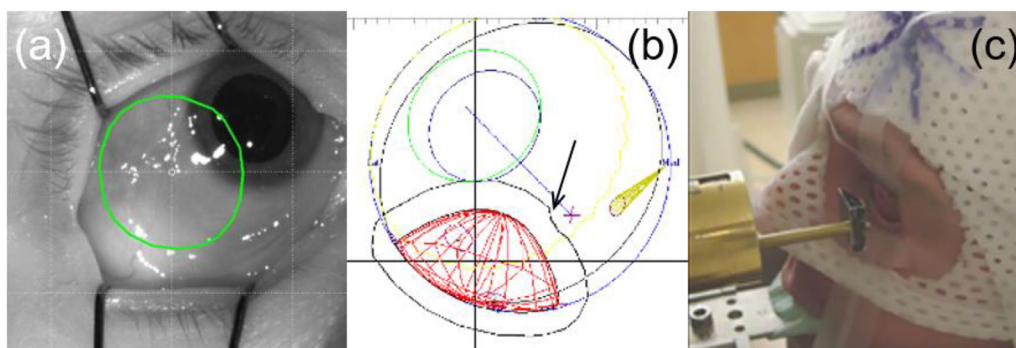


**Fig. 4.** Examples of treatment planning with normal tissue sparing techniques: (a) eyelid retraction and field confirmation (green contour); (b) macula notch (arrow) with local reduced aperture margin to spare dose on macula (purple cross); (c) wedge (arrow) or compensator (not shown) for beam shaping to reduce dose to critical structure (compare to Fig. 5).

outputs of the planning process are the collimator shape with wedge position (if needed), range and modulation of the proton beam, eye gaze angle, and corresponding positions of the clips for x-ray verification.

Preservation of the eye and vision is optimized by adjustments to lateral margin, aperture shape (Fig. 4b), distal range (Fig. 3f), gaze angle, and compensators or wedges (Figs. 3g, h and 4c). Critical structures should be systematically evaluated to minimize side effects, including the following: (1) posterior structures, ie, optic disc/nerve, macula, and retina; (2) anterior structures such as the lens, ciliary body, cornea, and the limbus/limbal stem cells; and (3) other tissues, ie, lacrimal gland, tear ducts, upper eyelid and eyelashes, lower eyelid (Fig. 4a), and bony orbit.<sup>81</sup> Noteworthy is the approach to automate the selection of gaze angle.<sup>82</sup>

Dose volume histogram (DVH) parameters are important for planning optimization and complication risk prognostication for patients. Multiple reports identify the volume of the macula and optic nerve length receiving 50% of the total dose (“V50%” or ~28-30 Gray equivalent) as independent predictors of post-OPT vision loss.<sup>83-85</sup> Importantly, if one of either the macula or optic disc can be relatively spared, despite the other receiving a higher dose, there may be a vision preservation advantage.<sup>83</sup> Hence, the dosimetric benefits of tight penumbra and selection of planning/delivery techniques are essential for vision preservation. Notched aperture beams can reduce the dose to the optic disc, macula, or nerve (Fig. 4b).

DVH analysis and planning modifications for ciliary body and optic disc/nerve dose can also be used to reduce risk of neovascular glaucoma. Similarly, the lens dose is modified to minimize cataract risk.<sup>83-85</sup>

It should be noted that the historical data combine patient follow-up and DVH data coming from practically a single planning system, which describes individual anatomic structures using simple geometric representations. To what extent these data are representative in the context of modern 3D planning systems where individual structures are segmented based on 3D imaging is not clear.

Using a sharp distal beam fall-off, ciliary body and iris tumors can be treated without dose to the optic disc/macula

(Fig. 3f). Wedge filters may be used to reduce the disc dose or treatment dose volume (Fig. 3h). Dilating drops may be used to reduce the target area for iris melanomas. Limbal stem cell transplantation has been studied for whole anterior segment irradiation when treating extensive iris seeding.<sup>86,87</sup>

The gaze angle selection and systematic eyelid retraction techniques are critical to reducing long-term eyelid toxicity and potential keratinization of the upper palpebral conjunctiva (Fig. 4a). Transpalpebral treatment may also be used strategically.<sup>88</sup> Gaze angle may be further optimized to reduce dose to the lacrimal gland, tear duct, and other structures.

## OPT Delivery

### Dedicated low-energy, dedicated high-energy, and nondedicated delivery systems

The vast majority of ocular treatments over the past 4 decades have been performed by a small number of pioneering OPT centers with accelerators and beamlines specifically adapted for ocular therapy. These included dedicated high- and low-energy proton machines, the latter providing the sharpest physical dose characteristics due to minimal degradation and personalized collimation, with sufficient beam current for short treatment times of <1 minute.

Given the rarity of indications treated with OPT, the cost of a fully dedicated solution, as well as the absence of vendors of modern low-energy clinical machines and the departure of vendors of dedicated eyelines in high-energy proton systems, has led to debate on the future of ocular beam provision, especially since several older treatment accelerators are approaching obsolescence.

Newly emerging centers, when they decide to offer a solution for OPT, either opt for a dedicated nozzle coupled with the high-energy accelerator, or adapt ocular nozzles to high-energy proton gantries, accompanied by couch or inclined set-up, with on-board imaging<sup>80,89</sup> to make their delivery system more universal and suitable for performing this specialized treatment.

The use of high-energy proton beams for the treatment of intraocular tumors requires the deceleration of the protons, resulting in an increased distal fall-off and lateral penumbra (Table 2).<sup>90,91</sup> This results in reduced conformity, which in turn leads to potentially increased collateral damage and radiation side effects, as shown in silico.<sup>33</sup>

In our survey, we have collected information on the lateral penumbra and the distal fall-off from 5 dedicated low-energy systems and 14 high-energy systems (Table 2). The median reported distal fall-off is 1.0 mm (0.9-1.2 mm) for the low-energy systems and 2.8 mm (1.5-6.0 mm) for the high-energy systems. The values in parentheses indicate the range of reported values. Similarly, the median lateral penumbra is 1.4 mm (1.2-1.9 mm) and 1.6 mm (1.2-3.0 mm) for the low- and high-energy systems, respectively. These figures indicate that there are significant differences in the dosimetric characteristics of the high-energy solutions, and at the same time that the beam degradation of the high-energy systems can be partially mitigated by careful design, as some of the high-energy solutions achieve beam parameters that are not far from those of the dedicated low-energy systems, although the method of energy selection involves a significant loss of beam fluence with a consequent increase in treatment times.

A critical aspect to be addressed in the future is how changes in distal/lateral penumbra, dose inhomogeneity, range uncertainty, choice of beam angle, and clip placement may affect normal tissue dosing and resultant eye loss, vision changes, retinopathy, glaucoma, eyelid effects, and other clinical outcomes, since almost all of the clinical evidence is based on follow-up of patients treated with the dedicated OPT systems. Therefore, beam parameters play a critical role in the advancement of ocular treatments on universal beamlines.

## Beam generation

The following types of accelerators can provide proton beams for ocular therapy: (1) low-energy isochronous cyclotrons (60-74 MeV) formerly used for neutron therapy and research, with dedicated eyelines developed in-house, (2) high-energy isochronous cyclotrons (Varian ProBeam, IBA Proteus 235), (3) high-energy synchrocyclotrons (eg, IBA S2C2, Mevion S250i), and (4) synchrotrons, which provide selectable energies down to 70 MeV (eg, Hitachi-V ProBeat 250, Optivus, Siemens). Synchrocyclotrons, however, may provide reduced dose rates and prolong OPT treatment. A proton linac, with selectable energies from 70 to 200 MeV, is in development and offers a small footprint with narrow beam emittance (AVO-Light).

Most of OPT centers are currently located within hospital centers or clinical research institutes. Table 2 provides an overview of different eye treatment room configurations. These include the following: (1) a dedicated room solely for eye treatment, eg, Charité-HZB (Fig. 5a), Clatterbridge Cancer Centre (CCC), University of California San Francisco (UCSF), and Paul Scherrer Institute (PSI); (2) a shared gantry room with a nozzle adapted for eye therapy, as in the

case of Seattle Cancer Care Alliance (SCCA) (Fig. 5b); and (3) a shared room that accommodates another treatment line, as illustrated in Figure 5c, at the West German Proton Therapy Center Essen (WPE).

More than half of operational OPT systems have been developed “in house,” eg, Massachusetts General Hospital (MGH), UCSF and Institut Curie Proton Therapy Center Orsay (ICPO), and a minority by commercial vendors eg, the University of Florida Health Proton Therapy Institute (UFHPTI) and WPE eye-line by IBA, HollandPTC in Delft by Varian. Most ocular OPT systems use a spinning range-modulator wheel (propeller) to generate the spread-out-Bragg-peak (SOBP) with the number in wheel libraries varying between centers, eg, 12 at UFHPTI, 40 at MGH, and >90 at CCC. Alternative methods for SOBP generation include active energy selection/energy stacking with an optional ridge filter (SCCA, Centro Nazionale di Adroterapia Oncologica (CNAO)). Final range adjustment is achieved by intercepting the beam with a discrete range shifter (eg, plates of varying thicknesses or rotating wheel with discrete steps) or continuous range shifter, for example, a variable water column (at UCSF<sup>18</sup>), a selectable wedge, or smoothly varying thickness wheel.

Experience has shown that the useful energy range for OPT is from 65 to 75 MeV (from 36 to 46 mm in water), which would encompass the deepest tumors, overlying tissue, depth margins, and compensator thicknesses. Obtaining ocular treatment energies with high-energy accelerators is either by the absorber and slits of the energy selection system (ESS) or by machine adjustment (eg, synchrotron or proton linac). The latter systems still require the use of fine range-shifters in the eyeline to achieve the prescribed range. The resolution of energy adjustments depends on vendor or in-house design, informed by local clinical preferences.

Increased beam ranges (>36 mm) are available from degraded high-energy gantry beams and some fixed horizontal lines, opening the possibility of using lateral beam treatments through the zygomatic bone. Multiple anterior fields are being planned to reduce anterior dose and improve planning “robustness” but must be weighed against longer treatment times and potential side effects from multiple anterior and lateral beam entrance doses. Dose “shadow” behind the clips anterior to the tumor volume should be taken into consideration.<sup>92</sup> Optimization of treatment isodoses by multiple gantry fields is being investigated at NWMPC (Chicago)<sup>78</sup> along with the use of anatomic landmarks for set-up positioning. Tumor control, eye preservation, vision loss, and patient-centered functional and aesthetic quality of life outcomes will need to be compared across proton beamlines to fully understand the benefits and costs of adapting different systems.

## Beam shaping

Collimators and compensators are costly to produce as they are patient-specific. Apertures of 30 to 35 mm maximum



**Table 2 Ocular Proton and Carbon Therapy centers, with machine, beam, and treatment room characteristics (from Schalenbourg and Zografos,<sup>32</sup> personal communications, OPTIC QA Survey)**

Centers; first treatment year	Vendor	Accelerator type	Accelerator energy (MeV)	Room energy (MeV)	Beam type	Treatment room	Distal fall-off at 90%-10% (mm) * in water	Lateral penumbra at 80%-20% (mm)* in water	Room configuration
MGH (HCL/ F Burr), Boston, USA (1975/ 2001)	HCL/IBA	Isochronous cyclotron	230	159	Degraded; continuous; passive-scattering	Shared room	6.0	1.5	Horizontal fixed beam; chair
PSI (OPTIS2), Villigen, Switzerland (1984)	Accel-Varian	Isochronous SC cyclotron	250	70	Degraded; continuous; passive-scattering	Dedicated room, shared beam	1.5	1.6	Horizontal fixed beam; chair
CCC, Wirral UK (1989)	Scanditronix (MC62 P)	Isochronous cyclotron	62.5	60.1	Continuous; passive-scattering	Dedicated room, dedicated beam	1.0	1.3	Horizontal fixed beam; chair
LLUMC, Loma Linda, USA (1990)	Optivus Proton Therapy Inc	Synchrotron	250	100 <sup>†</sup>	Degraded; pulsed; passive-scattering	Shared room, shared beam	2.6	1.6	Horizontal fixed beam; chair
CAL, Nice, France (1991)	MEDICYC-Consortium	Isochronous cyclotron	65	62.5	Continuous; passive-scattering	Dedicated room, dedicated beam	1.0	1.4	Horizontal fixed beam; chair
ICPO-Curie, Orsay France (1991)	IBA; Proteus Plus	Isochronous cyclotron	230	75	Degraded; continuous; passive-scattering	Shared room, shared beam	2.8	1.6	Horizontal fixed beam; chair
UCSF, San Francisco, USA (1994)	Crocker Nuclear Laboratory	76-inch, 4-sector cyclotron	67.5	59.2	Continuous; passive scattering	Dedicated room, dedicated beam	1.2	1.5	Horizontal fixed beam; chair
HZB-Charité, Berlin, Germany (1998)	Scanditronix; K-130	Isochronous, 4-sector cyclotron	72	64.7	Continuous; passive scattering	Dedicated room	1.0	1.9	Horizontal fixed beam; chair
INFN-LNS, Catania, Italy (2001)	LASA, Milan; K-800	Isochronous, 3-sector SC cyclotron	62	60	Continuous; passive scattering	Dedicated room; shared beam	0.9	1.2	Horizontal fixed beam; chair
NIRS, Chiba, Japan (1986-	HIMAC	Synchrotron	140 or 170 MeV/u	-		Shared room; shared beam	2.3	4.0	Fixed horizontal and vertical beams,

(Continued)

**Table 2** (Continued)

Centers; first treatment year	Vendor	Accelerator type	Accelerator energy (MeV)	Room energy (MeV)	Beam type	Treatment room	Distal fall-off at 90%-10% (mm) * in water	Lateral penumbra at 80%-20% (mm)* in water	Room configuration
2003 protons), (2001 carbon ions only)					Carbon beam; pulsed; passive scattering with wobbling				ocular nozzle, couch
NCC, Seoul, Korea (2009)	IBA; Proteus 235	Isochronous cyclotron	230	60	Continuous; degraded by ESS; passive-scattering	Shared room, shared beam	4.4	1.7	Fixed beam and gantry with ocular nozzle; couch
NWPC, Chicago, USA (2011)	IBA; Proteus Plus	Isochronous cyclotron	230	-	Continuous; degraded by ESS, uniform scanning	Shared room; shared beam	3.4	2.0	Fixed horizontal or inclined line or gantry with ocular nozzle
IFJ/BCC, Krakow, Poland (2011)	IBA; Proteus Plus	Isochronous cyclotron	235	70	Degraded by ESS; continuous; passive-scattering	Dedicated room	1.6	1.2	Horizontal fixed beam; chair
SCCA, Seattle, USA (2016)	IBA; Proteus Plus	Isochronous cyclotron	235	63-90	Degraded by ESS; pencil beam	Shared room; shared beam	3.0	3.0	Gantry beam with eye nozzle; couch and chair
UFPTI, Florida, USA (2012)	IBA; Proteus Plus	Isochronous cyclotron	230	105	Degraded by ESS; continuous; passive scattering	Dedicated room; shared beam	3.0	1.2	Horizontal fixed beam; chair
CNAO, Pavia, Italy (2016)	PIMMS Consortium	Synchrotron	229	62-90 <sup>†</sup>	Degraded; Pulsed; pencil beam scanning	Shared room	1.5	1.4	Horizontal beam; inclined couch and chair
SPHIC Shanghai, China (2018)	Siemens: Iontris	Synchrotron (protons and C ions)	250 (p); 430 (C)	70 (p) <sup>†</sup> ; 85 (C)	Machine adjustable; pulsed; pencil/raster beam; ridge filter	Shared room; shared beam	2.0 (p) <sup>†</sup> ; n.a. (C)	1.3 (p) <sup>†</sup> ; n.a. (C)	Horizontal and vertical beams; chair
HollandPTC, Delft, Netherlands (2020)	Varian; ProBeam	Isochronous SC cyclotron	250	75	Degraded; continuous; passive-scattering	Dedicated room; shared beam	2.8	1.7-2.2	Horizontal beamline; chair
WPE, Essen, Germany (2021)	IBA; Proteus Plus	Isochronous cyclotron	235	82.5	Degraded; continuous; pencil beam	Shared room	2.0	1.3-1.4	Horizontal beamline; chair
		Synchrotron	228	71 <sup>†</sup>		Shared room	-	-	

(Continued)

**Table 2** (Continued)

Centers; first treatment year	Vendor	Accelerator type	Accelerator energy (MeV)	Room energy (MeV)	Beam type	Treatment room	Distal fall-off at 90%-10% (mm) * in water	Lateral penumbra at 80%-20% (mm)* in water	Room configuration
Mayo Clinic, Rochester, Minn. USA (2022)	Hitachi; ProBeat-V				Machine adjustable; pulsed, pencil beam				Gantry beam with eye nozzle; couch and chair

The beam data are for typical clinical SOBP beams.  
 Abbreviations: EES = energy selection system; SC: superconducting main magnet; SOBP = spread-out-Bragg-peak.  
 \* Data obtained from literature and personal communications, carbon beam in development.  
 † Selected by synchrotron energy adjustment.

diameter are common, which balance field uniformity with a sufficient dose rate. Patient-specific brass collimators are universally employed but are labor-intensive and require special disposal procedures. Microleaf collimation, although technically possible, is not available at present. Mesh or *microhole* collimators for “spatially” fractionated proton therapy have been fabricated at Institute of Nuclear Physics of Polish Academy of Sciences (IFJ PAN) (Kraków) and aim to reduce anterior dose and eyelid toxicity.<sup>3</sup> Three-dimensional printed collimators and compensators (polylactic acid) have been developed at the Mayo Clinic PTC.<sup>3</sup> The gantry-adapted systems, using several individual pencil beams, offer wider diameter fields of between 40 and 60 mm, which are suitable for conjunctival tumors and avoid the need for field *patching*. Pencil beam scanning beams are employed at most high-energy vendor systems, where a single beam covers or “scans” an aperture or if required, a larger field is obtained by scanning using several “adjacent” pencil beams. However, the dose fall-off and penumbrae with pencil beam scanning beams for ocular tumors are generally wider than those produced by dedicated beamlines due to beam energy and fluence degradation in the ESS, the size and proximity of the nozzle range absorbers (Table 2).<sup>74,75</sup> Similarly, dose rate, hence treatment time, is affected by the low efficiency of the cyclotron ESS. Wedges are located on the patient collimators and are made of polymethyl methacrylate (PMMA) or aluminum (Fig. 4c). They are employed by a third of the centers, to spare posterior tissue and reduce the dose volume. These are particularly effective when used with sharply conformal isodoses. Aperture fields may also have small “notches” that are created by small bulges on the collimator; these have been shown to offer very localized dose sparing at the optic disc and macula (Fig. 4b).<sup>10</sup>

**Patient set-up**

Most proton ocular centers at present use a similar planning and beam delivery technique. The immobilization and beamline system used an upright patient treatment configuration with a dedicated fixed proton beam line, although supine or inclined treatment couches are used at 3 centers (see Table 2). Chair and headframe movement adjustments include standard orthogonal planes, pitch, and yaw corrections. All centers use orthogonal digital panels for x-ray imaging for simulation and patient positioning, although configurations differ. Patient participation is fundamental in minimizing side effects from proton radiation by maintaining a selected gaze direction, which has been optimized during the planning process. If vision is impaired before treatment, the contralateral eye can be used for gaze fixation, with clinical assessment required to confirm positioning and conjugate gaze.

Eyelid retraction (Fig. 4a) is clinically relevant to the short- and long-term effects of erythema, scarring, eyelash alopecia, keratinization, aesthetics, and quality of life. For small and medium tumors, most if not all the eyelids can be successfully

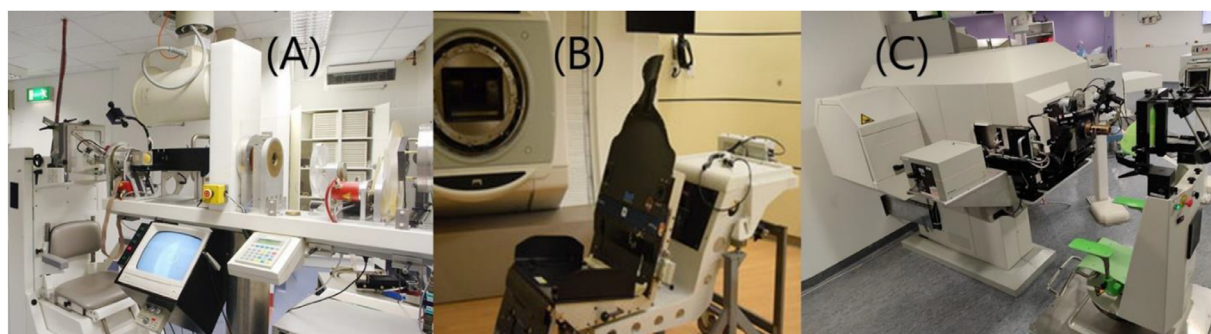


**Fig. 5.** Ocular Therapy facilities: (A) low-energy facility with dedicated treatment room at Charité-HZB; (B) adapted gantry line SCCA; and (C) dedicated eye nozzle for a degraded beam in a shared room configuration at WPE.

retracted outside of the field by a combination of clinical expertise, variable/multiple retractors, head tilt, and chair rotation adjustment. For larger tumors, the upper eyelid is, by preference, fully retracted to minimize lid keratinization, alternatively a transpalpebral technique may be employed.<sup>81,88</sup>

Patient set-up, although an iterative and invasive process, is extremely accurate, with submillimetric precision reported by the OPT institutions. Eye motion monitoring during irradiation is based on closed-circuit television camera viewing of the treatment eye, with infrared lighting for improved contrast. Proton therapy centers with established and dedicated eye treatment programs have average annual throughputs from 100 to 300 patients (eg, CAL-Nice, Charité-HZB, CCC, Curie-Orsay, MGH, PSI, UCSF). Gantry beamlines, adapted with “eye” nozzles, are expected to have smaller patient throughput but may increase treatment access due to the greater availability of proton gantries with reduced travel time.

## Dosimetry and quality assurance

The exceptionally sharp conformal beam characteristics of ocular ion beams (Table 2), narrow fields, submillimetric range prescription, as well as the linear energy transfer quenching phenomenon at the Bragg peak, make significant demands on quality assurance (QA) procedures.<sup>90</sup> An overview of the current QA and dose calibration practices was obtained from a recent survey of current practices conducted at 15 institutions, operating ocular particle therapy.<sup>3</sup> The differences in proton therapy beamline design and accelerator characteristics are reflected in the type and frequency of adopted QA procedures (Table 3). Daily verification of a machine’s beam output and beam range is performed at most centers. SOBPs and lateral profiles are verified daily by half of the centers, with the rest at weekly or monthly intervals. The duration of daily QA at centers varies from <15 minutes to more than an hour.

Five centers measure their proton depth doses (range and SOBP) with a commercial phantom, for example, the QUBE multilayer ionization chamber (DETECTOR) at the proton therapy center in Orsay (ICPO), or an adapted commercial device from RT. Ten of the centers use custom-made devices

**Table 3** Summary of type and frequency of quality assurance procedures in ocular proton therapy obtained from the International Ocular Dosimetry Survey (2022)

Test	Frequency (no. of centers)		
	Daily	Weekly	Monthly
Dose or output constancy	93% (14)	20% (3)	0% (0)
Range of energy constancy	80% (12)	27% (4)	7% (1)
Shape of SOBP	47% (7)	27% (4)	13% (2)
Lateral profile (flatness and symmetry)	33% (5)	20% (3)	20% (3)
Dose rate or treatment time	36% (5)	21% (3)	0% (0)
Dose rate or MU dependence	14% (2)	7% (1)	0% (0)
Coincidence of x-ray and proton isocenter	13% (2)	13% (2)	33% (5)
Coincidence of light and proton field	13% (2)	7% (1)	27% (4)
Laser alignment with isocenter	40% (6)	20% (3)	20% (3)
Safety interlocks	71% (10)	7% (1)	7% (1)

*Abbreviation:* SOBP = spread-out-Bragg-peak.

(eg, multilayer ionization chamber at MGH; “baby Blue” phantom (IBA-Dosimetry) and a small “horizontal” water phantom at UFHPTI, parallel-plate ion chamber or diode with PMMA/Perspex wheel at most other centers. A novel and rapid daily range-verification method (at UCSF<sup>3</sup>) uses a 3D printed cone phantom backed with radiochromic film, which simultaneously indicates (in <5 minutes) proton range and x-ray-to-beam coincidence, resolved to within 0.1 and 0.2 mm, respectively. These devices are described in PTCOG OPTIC symposium YouTube channel<sup>2</sup> and website.<sup>3</sup>

By contrast, commercial devices are used for lateral beam profiles at half of the centers, which include radiochromic film, 3D water phantoms, and scanning diodes (eg, PTW and IBA). The Lynx 2D scintillator detector (IBA-Dosimetry) is used to verify profile flatness, symmetry, and proton

light-field coincidence at ICPO. Devices developed in-house have achieved high precision and were economical to develop, but now need to match the compactness, ease-of-use, fast acquisition, and data analysis available in commercial systems.

The International Atomic Energy Agency TRS-398 Code of Practice for Dosimetry<sup>93</sup> is followed by all but one of the survey respondents, although the choice of ion chamber (parallel-plate, cylindrical ionization, or both) and measurement medium (eg, water and plastic) is varied. There are differences in the beam output (clinical monitor units (MU)) determination for each patient field. An ionization-chamber measurement in a custom-made plastic phantom provides a quick dose verification in a reference field, whereas some centers (5 of 15) measure in water or with patient aperture (3 of 15), or determine MU using an analytical model, look-up table, database or the TPS. Most centers (13 of 15) apply a constant relative biological effectiveness factor of 1.1 to convert the physical dose to the prescription dose, and one carbon center uses TPS-calculated relative biological effectiveness. Linear energy transfer depth corrections were not employed at any center.

American Association of Physicists in Medicine task group (TG) reports do not specifically include OPT, but their methodology has proved invaluable. The TG-100<sup>94</sup> offers a “Failure Mode and Effect Analysis” for continuous QA improvement, such as identifying as high-risk, those treatments that use light-fields instead of x-ray alignment, necessitating the implementation of additional cross-checks. The TG-224<sup>95</sup> report recommends the comprehensive proton therapy machine QA for both passive-scattering and scanning beam systems, but the suggested tolerances ( $\pm 1$  mm) are not suitable for the precision required in OPT. The TG-275<sup>96</sup> establishes effective review procedures, including checklists for chart review by therapy staff, with automation in plan checking. This has motivated some centers to develop patient-specific QA application software which selects the appropriate range-modulator wheel to match a patient-prescribed range and modulation, handles file transfer to the machine shop for aperture milling and predicts the MUs for a planned field.<sup>2,3</sup>

A large staff group ensures good service robustness and continuity, but if only a small fraction of staff time is dedicated to eye treatments, this may be a challenge to safer and consistent QA practice. The large variation in QA techniques makes the case for closer collaboration, standardization, and the adoption of the most effective techniques. It is hoped that the clarification of QA specifications will influence the equipment vendors to develop QA products that are specific to OPT.

## Post-OPT Care Best Practices

Although definitive OPT achieves high local control rates,<sup>4,14-16,19,22,23</sup> there are numerous potential clinical complications that can occur. These include inflammation

and irritation of the eyelid, permanent loss of eyelashes, scleral telangiectasias, occlusion of the tear duct, dry eyes, cataracts, pseudorecurrence (tumor inflammatory response), neovascular proliferation, secondary glaucoma, retinopathy, maculopathy, and optic neuropathy.<sup>31,47,97-100</sup> More severe toxicities from radiation treatment are generally rare, including corneal limbal stem cell failure, necrosis of the eyelid or sclera,<sup>101,102</sup> and exudative retinal detachment. Short-term surgical complications include perforation, diplopia, and postoperative hemorrhage. Tantalum markers can cause conjunctival granuloma.

Although most patients are adults, specific attention to treatment toxicity is also given to adolescent and young adult (AYA) patients to optimize the management of UM in this subpopulation. Specific understanding of AYA experience is reported by PSI where between 1997 and 2007, a total of 272 AYA (aged <40 years) patients were identified, and an additional 1984 adult patients were also treated.<sup>103</sup> Despite the excellent local control of tumors, nontrivial treatment complications included vision loss from neovascular glaucoma, maculopathy, optic neuropathy, retinopathy, cataracts, and dry eyes. Nearly 50% of AYA patients have tumors that are either near the optic disc or macula. Some of these patients retain vision despite the high-dose RT. Select patients are eligible for anti-vascular endothelial growth factor (anti-VEGF) therapy.

With the significant toxicity trade-offs of treatment, there is motivation toward developing more personalized and accurate eye and tumor models that integrate MRI and fundus photography in hopes of delivering still more conformal RT with fewer long-term side effects. Because toxicities of RT are predictable based upon treatment plans,<sup>83,104-106</sup> several strategies as described above in the surgical procedures, treatment planning, and delivery can be implemented to reduce critical structure dose and sequelae.

Specifically, toxic tumor syndrome can be treated by laser ablation or transscleral or transretinal ablation of the irradiated tumor and prevented by antiangiogenic therapy. Many of the severe inflammatory toxicities of RT can be successfully treated with steroids, anti-VEGF therapy,<sup>98</sup> vitrectomy, or endoresection<sup>107</sup> as appropriate, but sometimes enucleation is necessary. Some teams use prophylactic anti-VEGF therapy, for example,  $1 \times / 2$  months for 6 months then  $1 \times / 3$  months to reduce neovascularization of the anterior segment.<sup>108</sup> Neovascular glaucoma treatments include anti-VEGF and laser treatment once the ischemic retina is reattached. For radiation maculopathy, anti-VEGF therapy can be used to attempt to preserve vision and microcirculation. Angio-ocular coherence tomography may improve delineation of the foveal avascular zone.<sup>109</sup> Conjunctival granulomas are easily corrected by clip removal.

Local failures for UM and conjunctival tumors have been (re)treated with proton therapy. The ocular preservation rate after UM reirradiation is 40% at 5 years and visual acuity preservation of  $\geq 20/200$  in 30% of patients,<sup>22,29,30</sup> which offers an effective salvage as compared with enucleation. Further studies are necessary and with increased awareness

has come greater consideration of screening for early diagnosis, identifying unique populations such as young adults, and exploring new modalities such as targeted therapies and immunotherapies.

### Comparison with different radiation modalities

Comparative analyses between protons and other radiation modalities are limited by selection bias. Meta-analyses and systematic reviews show that plaques, as opposed to protons, are generally used for tumors with smaller base and/or height and tumors away from the optic disc/macula.<sup>4,110</sup> Short- and long-term local control rates are generally higher for charged particles when compared with plaque brachytherapy.<sup>4,5,111</sup> In these studies, proton treatment outcomes are represented by follow-up of patients treated exclusively with the dedicated low-energy systems.

Although the “least often used” form of treatment,<sup>112</sup> stereotactic RT is provided in regions where established techniques are lacking and/or due to patient circumstances. Normal tissue dosing and vision outcomes have been noted to be favorable after OPT versus other RT modalities for comparable tumors.<sup>113-115</sup> Proton therapy has been shown to result in lower radiation retinopathy rates, most likely due to a more uniform dose distribution and lower doses to smaller retinal volumes overall.<sup>110</sup> Reported short- and long-term local control rates for these techniques are more variable.<sup>116-118</sup> Table 4 gives an overview of tumor control and eye preservation after 5 years in UM for different irradiation modalities.

Anterior eye complications are more common with proton beam delivery than other radiation modalities. These are decreasing with contemporary OPT techniques in planning, dosing, delivery, and advances in expert ophthalmologic care.<sup>24,106,119</sup>

Of note, a cost-analysis study in the United States showed that short course OPT (4-5 fractions) may be more cost-effective than plaque brachytherapy based on the

current insurance schema.<sup>114</sup> This is not representative globally as the costs of treatment and its reimbursement seem to depend strongly on national health priorities and availability of plaques. Relative costs, with plaques or photon-based stereotactic radiation therapies, due to retinopathy, clinic visits, vision loss, and other adverse effects are under study and may also impact cost-effectiveness.<sup>110</sup>

In clinical practice, however, the choice of treatment modality is also dependent on the patient’s preferences, with the local availability of the modality often playing a significant role.

### Future Directions and Conclusions

In continuing to pioneer excellence in care for ocular patients, the most important developments require improved imaging modalities, TPS, QA techniques, and vendor options for low and high-energy beamlines, minimizing parameters such as lateral penumbra and distal fall-off and improving dose homogeneity and dose-rate. The 2022 Second International Survey of ocular proton centers provided a consensus on the most critical aspects of ongoing development and future research, which are as follows (Table 5):

- (1) Development of a commercially available and sustainable TPS;
- (2) Development of MRI imaging and fusion for target and normal tissue delineation in treatment planning;
- (3) Development of improved QA devices and standardization of practice;
- (4) Increased access to OPT.

In addition, eye tracking and gating during irradiation, multi-institutional outcomes studies, clipless technique, biologic treatment planning, multibeam and gantry-based options, ultrahigh dose rate (FLASH irradiations), and other particles (helium and carbon) were also noted to be important for future study.

Because of the relatively low demand and the specific technical requirements that need to be met, there is a limited availability of dedicated ophthalmic proton therapy systems in the industrial market. Therefore, advancements in this field require finding a compromise between optimizing parameters, ensuring availability, and managing costs within commercial systems. This approach aims to provide an effective solution for treating ocular diseases using proton therapy while considering the limitations and constraints of the current market. However, the excellent results achieved in the past with protons at dedicated irradiation facilities should not be uncritically transferred to facilities with other proton qualities and it should be evaluated whether the new solutions can confirm the excellent results achieved with the dedicated systems.

Higher linear energy transfer particles, such as helium and carbon, have shown similar local control rates to OPT<sup>5</sup> but their sharper physical characteristics suggest clinical

**Table 4 Overview of tumor control and eye preservation after 5 years of different irradiation modalities: proton therapy (protons), brachytherapy using ruthenium-106 (Ru-106) or iodine-125 (I-125) plaques, fractionated stereotactic radiation therapy (LINAC [SRT]) and single fraction radiosurgery (CyberKnife [SRS])**

Irradiation modality	Tumor control (after 5 y)	Eye preservation (after 5 y)	References
Protons	90%-99%	>90%	4,14,23,42
Ru-106	80%-98%	>90%	4,43
I-125	82%-99%	~90%	4,44
LINAC (SRT)	85%-96%	~78%	4,41
CyberKnife (SRS)	71%-84%	~81%	39,40

Abbreviation: SRT = stereotactic radiation therapy; SRS = stereotactic radiosurgery.

**Table 5** Survey results on future outlook: “How do you rank the importance of the following developments to improve ocular particle therapy? (1-5)”

	Most important (1)	Very important (2)	Important (3)	Not very important (4)	Not important at all (5)	Weighted average
TPS development	8	6	3	0	0	1.7
MRI imaging for target delineation	5	7	4	1	0	2.1
Development of QA devices/methods	2	9	6	0	0	2.2
Increased access to ocular proton therapy	4	4	7	2	0	2.4
Eye tracking/gating during irradiation	1	8	7	1	0	2.5
Multi-institutional outcome studies	3	5	7	2	0	2.5
Other development (1)*	1	1	1	1	0	2.5
Clipless treatments	1	3	9	4	0	2.9
Biological treatment planning (RBE/LET)	1	4	6	5	1	3.1
Multibeam/gantry-based treatments	1	4	5	5	2	3.2
FLASH (ultrahigh dose rate)	0	2	6	9	0	3.4
New particles (He, C, etc)	0	4	3	8	2	3.5
Grid therapy	0	1	5	9	2	3.7

*Abbreviations:* LET = linear energy transfer; MRI = magnetic resonance imaging; QA = quality assurance; TPS = treatment planning system.

advantage by offering decreasing integral and normal tissue doses, which will mitigate late effects.

Advancements in imaging integration may improve the quality and accuracy of derived eye models and eventually completely obviate the role of the fiducial clips in the definition of the target volume and potentially image-guided treatment. Although the high tumor control rates reported by the established centers indicate that there is little room for improvement in terms of tumor control, accurate models in combination with “sharp” beams and optimization of the full process can arguably play a positive role in reducing side effects associated with treatment.

The treatment of ocular tumors with protons and heavier charged particle techniques has been extensively and rigorously evaluated over decades of scientific work. This approach requires specific clinical and physics expertise and great care in the application, so that optimal local control and long-term eye preservation can be achieved. Acute and late ocular morbidity are dependent on patient, tumor and treatment parameters, thus, further clinical exploration of techniques and a combination of clinical modalities to maximize functional outcomes remain essential. Using a thoughtful approach, proton and other particle beam radiation can achieve high tumor control rates with the potential of preserving the eye and useful vision, optimizing the cost-benefit on the treatment of ocular tumors and maximizing patient quality of life. Substantial patient throughput and close cooperation between ophthalmology, RT, and medical physics are crucial for a successful OPT service.

## References

1. Particle Therapy Co-Operative Group (PTCOG). PTCOG website. Accessed July 23, 2024. <https://www.ptcog.ch/>.
2. PTCOG OPTIC. First International PTCOG Ocular Proton Therapy Symposium 2022 - YouTube channel. 2022. Accessed July 23, 2024. <https://www.youtube.com/playlist?list=PLx7XfOFbYilq2m d8L3ormJ0Z6zyuG-Rl>.
3. PTCOG OPTIC. First International PTCOG Ocular Proton Therapy Symposium 2022 - website. 2022. Accessed July 23, 2024. <https://indico.psi.ch/event/12099/>.
4. Chang MY, McCannel TA. Local treatment failure after globe-conserving therapy for choroidal melanoma. *Br J Ophthalmol* 2013;97:804-811. <https://doi.org/10.1136/bjophthalmol-2012-302490>.
5. Mishra KK, Quivey JM, Daftari IK, et al. Long-term results of the UCSF-LBNL randomized trial: Charged particle with helium ion versus iodine-125 plaque therapy for choroidal and ciliary body melanoma. *Int J Radiat Oncol Biol Phys* 2015;92:376-383. <https://doi.org/10.1016/j.ijrobp.2015.01.029>.
6. Courdi A, Caujolle JP, Grange JD, et al. Results of proton therapy of uveal melanomas treated in Nice. *Int J Radiat Oncol Biol Phys* 1999;45:5-11. [https://doi.org/10.1016/s0360-3016\(99\)00147-9](https://doi.org/10.1016/s0360-3016(99)00147-9).
7. Mosci C, Mosci S, Barla A, Squarcia S, Chauvel P, Iborra N. Proton beam radiotherapy of uveal melanoma: Italian patients treated in Nice, France. *Eur J Ophthalmol* 2009;19:654-660. <https://doi.org/10.1177/112067210901900421>.
8. Verma V, Mehta MP. Clinical outcomes of proton radiotherapy for uveal melanoma. *Clin Oncol (R Coll Radiol)* 2016;28:e17-e27. <https://doi.org/10.1016/j.clon.2016.01.034>.
9. Weber B, Paton K, Ma R, Pickles T. Outcomes of proton beam radiotherapy for large non-peripapillary choroidal and ciliary body melanoma at TRIUMF and the BC Cancer Agency. *Ocul Oncol Pathol* 2015;2:29-35. <https://doi.org/10.1159/000433546>.
10. Kacperek A. Protontherapy of eye tumours in the UK: A review of treatment at Clatterbridge. *Appl Radiat Isot* 2009;67:378-386. <https://doi.org/10.1016/j.apradiso.2008.06.012>.

11. Höcht S, Bechrakis NE, Nausner M, et al. Proton therapy of uveal melanomas in Berlin. 5 years of experience at the Hahn-Meitner Institute. *Strahlenther Onkol* 2004;180:419-424. <https://doi.org/10.1007/s00066-004-1222-5>.
12. Afshar AR, Stewart JM, Kao AA, Mishra KK, Daftari IK, Damato BE. Proton beam radiotherapy for uveal melanoma. *Exp Rev Ophthalmol* 2015;10:577-585. <https://doi.org/10.1586/17469899.2015.1120671>.
13. Cirrone GAP, Cuttneo G, Lojaco PA, et al. A 62-MeV proton beam for the treatment of ocular melanoma at laboratori nazionali del sud-INFN. *IEEE Trans Nucl Sci* 2004;51:860-865. <https://doi.org/10.1109/TNS.2004.829535>.
14. Egger E, Schalenbourg A, Zografos L, et al. Maximizing local tumor control and survival after proton beam radiotherapy of uveal melanoma. *Int J Radiat Oncol Biol Phys* 2001;51:138-147. [https://doi.org/10.1016/s0360-3016\(01\)01560-7](https://doi.org/10.1016/s0360-3016(01)01560-7).
15. Munzenrider JE, Verhey LJ, Gragoudas ES, et al. Conservative treatment of uveal melanoma: Local recurrence after proton beam therapy. *Int J Radiat Oncol Biol Phys* 1989;17:493-498. [https://doi.org/10.1016/0360-3016\(89\)90099-0](https://doi.org/10.1016/0360-3016(89)90099-0).
16. Gragoudas ES. Proton beam irradiation of uveal melanomas: The first 30 years. The Weisenfeld Lecture. *Invest Ophthalmol Vis Sci* 2006;47:4666-4673. <https://doi.org/10.1167/iov.06-0659>.
17. Damato B, Kacperk A, Chopra M, Campbell IR, Errington RD. Proton beam radiotherapy of choroidal melanoma: The Liverpool-Clatterbridge experience. *Int J Radiat Oncol Biol Phys* 2005;62:1405-1411. <https://doi.org/10.1016/j.ijrobp.2005.01.016>.
18. Char DH, Phillips T, Daftari I. Proton teletherapy of uveal melanoma. *Int Ophthalmol Clin* 2006;46:41-49. <https://doi.org/10.1097/OI.0000195853.85581.C0>.
19. Dendale R, Lumbroso-Le Rouic L, Noel G, et al. Proton beam radiotherapy for uveal melanoma: Results of Curie Institut-Orsay proton therapy center (ICPO). *Int J Radiat Oncol Biol Phys* 2006;65:780-787. <https://doi.org/10.1016/j.ijrobp.2006.01.020>.
20. Kodjikian L, Roy P, Rouberol F, et al. Survival after proton-beam irradiation of uveal melanomas. *Am J Ophthalmol* 2004;137:1002-1010. <https://doi.org/10.1016/j.ajo.2004.01.006>.
21. Fuss M, Loreda LN, Blacharski PA, Grove RI, Slater JD. Proton radiation therapy for medium and large choroidal melanoma: Preservation of the eye and its functionality. *Int J Radiat Oncol Biol Phys* 2001;49:1053-1059. [https://doi.org/10.1016/s0360-3016\(00\)01430-9](https://doi.org/10.1016/s0360-3016(00)01430-9).
22. Marucci L, Ancukiewicz M, Lane AM, Collier JM, Gragoudas ES, Munzenrider JE. Uveal melanoma recurrence after fractionated proton beam therapy: Comparison of survival in patients treated with reirradiation or with enucleation. *Int J Radiat Oncol Biol Phys* 2011;79:842-846. <https://doi.org/10.1016/j.ijrobp.2009.12.018>.
23. Seibel I, Cordini D, Rehak M, et al. Local recurrence after primary proton beam therapy in uveal melanoma: Risk factors, retreatment approaches, and outcome. *Am J Ophthalmol* 2015;160:628-636. <https://doi.org/10.1016/j.ajo.2015.06.017>.
24. Egger E, Zografos L, Schalenbourg A, et al. Eye retention after proton beam radiotherapy for uveal melanoma. *Int J Radiat Oncol Biol Phys* 2003;55:867-880. [https://doi.org/10.1016/s0360-3016\(02\)04200-1](https://doi.org/10.1016/s0360-3016(02)04200-1).
25. Egan KM, Gragoudas ES, Seddon JM, et al. The risk of enucleation after proton beam irradiation of uveal melanoma. *Ophthalmology* 1989;96:1377-1382. [https://doi.org/10.1016/s0161-6420\(89\)32738-2](https://doi.org/10.1016/s0161-6420(89)32738-2) discussion 1382-1383.
26. Middleton MR, McAlpine C, Woodcock VK, et al. Tebentafusp, a TCR/Anti-CD3 bispecific fusion protein targeting gp100, potently activated antitumor immune responses in patients with metastatic melanoma. *Clin Cancer Res* 2020;26:5869-5878. <https://doi.org/10.1158/1078-0432.CCR-20-1247>.
27. Barker CA, Salama AK. New NCCN guidelines for uveal melanoma and treatment of recurrent or progressive distant metastatic melanoma. *J Natl Compr Canc Netw* 2018;16:646-650. <https://doi.org/10.6004/jnccn.2018.0042>.
28. Bechrakis NE, Bornfeld N, Heindl LM, Skoetz N, Leyvraz S, Jousseaume AM. Uveal melanoma – standardised procedure in diagnosis, therapy and surveillance. *Klin Monbl Augenheilkd* 2021;238:761-772. <https://doi.org/10.1055/a-1534-0198>.
29. Caujolle JP, Paoli V, Chamorey E, et al. Local recurrence after uveal melanoma proton beam therapy: Recurrence types and prognostic consequences. *Int J Radiat Oncol Biol Phys* 2013;85:1218-1224. <https://doi.org/10.1016/j.ijrobp.2012.10.005>.
30. Riechardt AI, Cordini D, Dobner B, et al. Salvage proton beam therapy in local recurrent uveal melanoma. *Am J Ophthalmol* 2014;158:948-956. <https://doi.org/10.1016/j.ajo.2014.07.013>.
31. Damato B, Kacperk A, Errington D, Heimann H. Proton beam radiotherapy of uveal melanoma. *Saudi J Ophthalmol* 2013;27:151-157. <https://doi.org/10.1016/j.sjopt.2013.06.014>.
32. Csutak A, Lengyel I, Jonasson F, et al. Agreement between image grading of conventional (45°) and ultra wide-angle (200°) digital images in the macula in the Reykjavik eye study. *Eye (Lond)* 2010;24:1568-1575. <https://doi.org/10.1038/eye.2010.85>.
33. Schalenbourg A, Zografos L. Pitfalls in colour photography of choroidal tumours. *Eye (Lond)* 2013;27:224-229. <https://doi.org/10.1038/eye.2012.267>.
34. Nürnberg D, Seibel I, Riechardt AI, et al. Multimodal imaging of the choroidal melanoma, with differential diagnosis, therapy (radiation planning) and follow-up. *Klin Monbl Augenheilkd* 2018;235:1001-1012. <https://doi.org/10.1055/A-0667-0806>.
35. Ferreira TA, Jaarsma-Coes MG, Marinkovic M, et al. MR imaging characteristics of uveal melanoma with histopathological validation. *Neuroradiology* 2022;64:171-184. <https://doi.org/10.1007/s00234-021-02825-5>.
36. Jaarsma-Coes MG, Klaassen L, Verbist BM, et al. Inter-observer variability in MR-based target volume delineation of uveal melanoma. *Adv Radiat Oncol* 2022;8 101149. <https://doi.org/10.1016/j.adro.2022.101149>.
37. Via R, Pica A, Antonioli L, et al. MRI and FUNDUS image fusion for improved ocular biometry in Ocular Proton Therapy. *Radiother Oncol* 2022;174:16-22. <https://doi.org/10.1016/j.radonc.2022.06.021>.
38. Cennamo G, Romano MR, Velotti N, Breve MA, de Crecchio G, Cennamo G. Fundus autofluorescence of choroidal nevi and melanoma. *Acta Ophthalmol* 2018;96:e102-e104. <https://doi.org/10.1111/aos.13413>.
39. Shields CL, Lim LS, Dalvin LA, Shields JA. Small choroidal melanoma: Detection with multimodal imaging and management with plaque radiotherapy or AU-011 nanoparticle therapy. *Curr Opin Ophthalmol* 2019;30:206-214. <https://doi.org/10.1097/ICU.0000000000000560>.
40. Cennamo G, Romano MR, Breve MA, et al. Evaluation of choroidal tumors with optical coherence tomography: Enhanced depth imaging and OCT-angiography features. *Eye (Lond)* 2017;31:906-915. <https://doi.org/10.1038/eye.2017.14>.
41. Wulff J, Koska B, Heufelder J, et al. Commissioning and validation of a novel commercial TPS for ocular proton therapy. *Med Phys* 2023;50:365-379. <https://doi.org/10.1002/mp.16006>.
42. Cordini D. Einführung eines therapieplanungssystems für die protonentherapie von augentumoren in die klinische routine. 2017. [doi:10.17169/REFUBIUM-4675](https://doi.org/10.17169/REFUBIUM-4675).
43. Hrbacek J, Mishra KK, Kacperk A, et al. Practice patterns analysis of ocular proton therapy centers: The international OPTIC survey. *Int J Radiat Oncol Biol Phys* 2016;95:336-343. <https://doi.org/10.1016/j.ijrobp.2016.01.040>.
44. Daftari I, Mishra K, Seider M, Damato B. Proton beam ocular treatment in eyes with intraocular silicone oil: Effects on physical beam parameters and clinical relevance of silicone oil in EYEPLAN dose-volume histograms. *Int J Med Physics Clin Eng Radiat Oncol* 2018;7:347-362. <https://doi.org/10.4236/IJMP.2018.7.3029>.
45. Oxenreiter MM, Lane AM, Aronow MB, et al. Proton beam irradiation of uveal melanoma involving the iris, ciliary body and anterior choroid without surgical localisation (light field). *Br J Ophthalmol* 2022;106:518-521. <https://doi.org/10.1136/bjophthalmol-2020-318063>.



46. Willerding GD, Cordini D, Hackl C, et al. Proton beam radiotherapy of diffuse iris melanoma in 54 patients. *Br J Ophthalmol* 2015;99:812-816. <https://doi.org/10.1136/bjophthalmol-2014-305174>.
47. Gollrad J, Böker A, Vitzthum S, et al. Proton therapy for 166 patients with iris melanoma: Side effects and oncologic outcomes. *Ophthalmol Retina* 2023;7:266-274. <https://doi.org/10.1016/j.oret.2022.08.026>.
48. Via R, Hennings F, Fattori G, et al. Noninvasive eye localization in ocular proton therapy through optical eye tracking: A proof of concept. *Med Phys* 2018;45:2186-2194. <https://doi.org/10.1002/mp.12841>.
49. Via R, Hennings F, Fattori G, et al. Technical note: Benchmarking automated eye tracking and human detection for motion monitoring in ocular proton therapy. *Med Phys* 2020;47:2237-2241. <https://doi.org/10.1002/mp.14087>.
50. Via R, Fassi A, Fattori G, et al. Optical eye tracking system for real-time noninvasive tumor localization in external beam radiotherapy. *Med Phys* 2015;42:2194-2202. <https://doi.org/10.1118/1.4915921>.
51. Spaccapaniccia C, Via R, Thominet V, et al. Non-invasive recognition of eye torsion through optical imaging of the iris pattern in ocular proton therapy. *Phys Med Biol* 2021;66(13). <https://doi.org/10.1088/1361-6560/ac0afb>.
52. Dobler B, Bendl R. Precise modelling of the eye for proton therapy of intra-ocular tumours. *Phys Med Biol* 2002;47:593-613. <https://doi.org/10.1088/0031-9155/47/4/304>.
53. Pfeiffer K, Bendl R. Real-time dose calculation and visualization for the proton therapy of ocular tumours. *Phys Med Biol* 2001;46:671-686. <https://doi.org/10.1088/0031-9155/46/3/304>.
54. Heufelder J, Cordini D, Fuchs H, et al. Five years of proton therapy of eye neoplasms at the Hahn-Meitner Institute, Berlin. *Z Med Phys* 2004;14:64-71. <https://doi.org/10.1078/0939-3889-00190>.
55. Weber A, Cordini D, Stark R, Heufelder J. The influence of silicone oil used in ophthalmology on the proton therapy of uveal melanomas. *Phys Med Biol* 2012;57:8325-8341. <https://doi.org/10.1088/0031-9155/57/24/8325>.
56. Ferreira TA, Grech Fonk L, Jaarsma-Coes MG, van Haren GGR, Marinkovic M, Beenakker JM. MRI of uveal melanoma. *Cancers (Basel)* 2019;11:377. <https://doi.org/10.3390/cancers11030377>.
57. Foti PV, Travali M, Farina R, et al. Diagnostic methods and therapeutic options of uveal melanoma with emphasis on MR imaging-Part I: MR imaging with pathologic correlation and technical considerations. *Insights Imaging* 2021;12:66. <https://doi.org/10.1186/s13244-021-01000-x>.
58. de Graaf P, Görnicke S, Rodjan F, et al. Guidelines for imaging retinoblastoma: Imaging principles and MRI standardization. *Pediatr Radiol* 2012;42:2-14. <https://doi.org/10.1007/s00247-011-2201-5>.
59. Beenakker JW, Ferreira TA, Soemarwoto KP, et al. Clinical evaluation of ultra-high-field MRI for three-dimensional visualisation of tumour size in uveal melanoma patients, with direct relevance to treatment planning. *MAGMA* 2016;29:571-577. <https://doi.org/10.1007/s10334-016-0529-4>.
60. Jaarsma-Coes MG, Ferreira TA, Marinkovic M, et al. Comparison of magnetic resonance imaging-based and conventional measurements for proton beam therapy of uveal melanoma. *Ophthalmol Retina* 2023;7:178-188. <https://doi.org/10.1016/j.oret.2022.06.019>.
61. Via R, Hennings F, Pica A, et al. Potential and pitfalls of 1.5T MRI imaging for target volume definition in ocular proton therapy. *Radiother Oncol* 2021;154:53-59. <https://doi.org/10.1016/j.radonc.2020.08.023>.
62. Sepahdari AR, Politi LS, Aakalu VK, Kim HJ, Razek AA. Diffusion-weighted imaging of orbital masses: multi-institutional data support a 2-ADC threshold model to categorize lesions as benign, malignant, or indeterminate. *AJNR Am J Neuroradiol* 2014;35:170-175. <https://doi.org/10.3174/ajnr.A3619>.
63. Klaassen L, Jaarsma-Coes MG, Verbist BM, et al. Automatic three-dimensional magnetic resonance-based measurements of tumour prominence and basal diameter for treatment planning of uveal melanoma. *Phys Imaging Radiat Oncol* 2022;24:102-110. <https://doi.org/10.1016/j.phro.2022.11.001>.
64. Tang MCY, Ferreira TA, Marinkovic M, et al. MR-based follow-up after brachytherapy and proton beam therapy in uveal melanoma. *Neuroradiology* 2023;65:1271-1285. <https://doi.org/10.1007/s00234-023-03166-1>.
65. Foti PV, Longo A, Reibaldi M, et al. Uveal melanoma: quantitative evaluation of diffusion-weighted MR imaging in the response assessment after proton-beam therapy, long-term follow-up. *Radiol Med* 2017;122:131-139. <https://doi.org/10.1007/s11547-016-0697-3>.
66. Jaarsma-Coes MG, Klaassen L, Marinkovic M, et al. Magnetic resonance imaging in the clinical care for uveal melanoma patients-a systematic review from an ophthalmic perspective. *Cancers (Basel)* 2023;15:2995. <https://doi.org/10.3390/cancers15112995>.
67. Paul K, Huelnhagen T, Oberacker E, et al. Multiband diffusion-weighted MRI of the eye and orbit free of geometric distortions using a RARE-EPI hybrid. *NMR Biomed* 2018;31(3). <https://doi.org/10.1002/nbm.3872>.
68. Oberacker E, Paul K, Huelnhagen T, et al. Magnetic resonance safety and compatibility of tantalum markers used in proton beam therapy for intraocular tumors: A 7.0 Tesla study. *Magn Reson Med* 2017;78:1533-1546. <https://doi.org/10.1002/mrm.26534>.
69. Marnitz S, Cordini D, Bendl R, et al. Proton therapy of uveal melanomas: intercomparison of MRI-based and conventional treatment planning. *Strahlenther Onkol* 2006;182:395-399. <https://doi.org/10.1007/s00066-006-1512-1>.
70. Fleury E, Trnková P, Erdal E, et al. Three-dimensional MRI-based treatment planning approach for non-invasive ocular proton therapy. *Med Phys* 2021;48:1315-1326. <https://doi.org/10.1002/mp.14665>.
71. Goitein M, Miller T. Planning proton therapy of the eye. *Med Phys* 1983;10:275-283. <https://doi.org/10.1118/1.595258>.
72. Daftari IK, Mishra KK, O'Brien JM, et al. Fundus image fusion in EYEPLAN software: An evaluation of a novel technique for ocular melanoma radiation treatment planning. *Med Phys* 2010;37:5199-5207. <https://doi.org/10.1118/1.3488891>.
73. Ik Daftari, E Aghaian, O'Brien JM, Dillon W, Phillips TL. 3D MRI-based tumor delineation of ocular melanoma and its comparison with conventional techniques. *Med Phys* 2005;32:3355-3362. <https://doi.org/10.1118/1.2068927>.
74. Lane AM, Oxenreiter MM, Hashmi M, et al. A comparison of treatment outcomes after standard dose (70 Gy) versus reduced dose (50 Gy) proton radiation in patients with uveal melanoma. *Ophthalmol Retina* 2022;6:1089-1097. <https://doi.org/10.1016/j.oret.2022.05.006>.
75. Mishra KK, Daftari IK. Proton therapy for the management of uveal melanoma and other ocular tumors. *Chin Clin Oncol* 2016;5:50. <https://doi.org/10.21037/cco.2016.07.06>.
76. Wulff J, Koska B, Janson M, et al. Technical note: Impact of beam properties for uveal melanoma proton therapy-an *in silico* planning study. *Med Phys* 2022;49:3481-3488. <https://doi.org/10.1002/mp.15573>.
77. Rethfeldt C, Fuchs H, Gardey KU. Dose distributions of a proton beam for eye tumor therapy: Hybrid pencil-beam ray-tracing calculations. *Med Phys* 2006;33:782-791. <https://doi.org/10.1118/1.2168067>.
78. Hartsell WF, Kapur R, Hartsell SO, et al. Feasibility of Proton Beam Therapy for Ocular Melanoma Using a Novel 3D Treatment Planning Technique. *Int J Radiat Oncol Biol Phys* 2016;95:353-359. <https://doi.org/10.1016/j.ijrobp.2016.02.039>.
79. Gerard A, Peyrichon ML, Vidal M, et al. Ocular proton therapy, pencil beam scanning high energy proton therapy or stereotactic radiotherapy for uveal melanoma; an *in silico* study. *Cancer Radiother* 2022;26:1027-1033. <https://doi.org/10.1016/j.canrad.2022.03.003>.
80. Regmi R, Maes D, Nevitt A, et al. Treatment of ocular tumors through a novel applicator on a conventional proton pencil beam scanning beamline. *Sci Rep* 2022;12:4648. <https://doi.org/10.1038/s41598-022-08440-5>.
81. Mishra KK, Afshar AR, Scholey Jessica M, Kacperek A, Damato BE. Ocular malignancies. In: Malouff TD, Trifiletti DM, eds. *Principles and Practice of Particle Therapy*. John Wiley & Sons, Ltd; 2022:201-224. <https://doi.org/10.1002/9781119707530.ch14>.

82. Hennings F, Lomax A, Pica A, Weber DC, Hrbacek J. Automated treatment planning system for uveal melanomas treated with proton therapy: A proof-of-concept analysis. *Int J Radiat Oncol Biol Phys* 2018;101:724-731. <https://doi.org/10.1016/j.ijrobp.2018.02.008>.
83. Polishchuk AL, Mishra KK, Weinberg V, et al. Temporal evolution and dose-volume histogram predictors of visual acuity after proton beam radiation therapy of uveal melanoma. *Int J Radiat Oncol Biol Phys* 2017;97:91-97. <https://doi.org/10.1016/j.ijrobp.2016.09.019>.
84. Caujolle JP, Mammari H, Chamorey E, Pinon F, Hérault J, Gastaud P. Proton beam radiotherapy for uveal melanomas at nice teaching hospital: 16 years' experience. *Int J Radiat Oncol Biol Phys* 2010;78:98-103. <https://doi.org/10.1016/j.ijrobp.2009.07.1688>.
85. Thariat J, Grange JD, Mosci C, et al. Visual outcomes of parapapillary uveal melanomas following proton beam therapy. *Int J Radiat Oncol Biol Phys* 2016;95:328-335. <https://doi.org/10.1016/j.ijrobp.2015.12.011>.
86. Singh AD, Dupps WJ, Biscicli CV, et al. Limbal stem cell preservation during proton beam irradiation for diffuse iris melanoma. *Cornea* 2017;36:119-122. <https://doi.org/10.1097/ICO.0000000000001063>.
87. Leblanc A, Lumbroso-Le Rouic L, Desjardins L, Dendale R, Cassoux N. Diffuse iris melanoma: conservative treatment with proton beam therapy after limbal stem cell preservation or enucleation? *Ocul Oncol Pathol* 2019;5:396-401. <https://doi.org/10.1159/000496847>.
88. Konstantinidis L, Roberts D, Errington RD, Kacperek A, Heimann H, Damato B. Transpalpebral proton beam radiotherapy of choroidal melanoma. *Br J Ophthalmol* 2015;99:232-235. <https://doi.org/10.1136/bjophthalmol-2014-305313>.
89. Saini J, Maes D, Regmi R, et al. Improved lateral penumbra for proton ocular treatments on a general-purpose spot scanning beamline. *Phys Med* 2023;107:102551. <https://doi.org/10.1016/j.ejmp.2023.102551>.
90. Kacperek A. Ocular proton therapy centers. In: Linz U, ed. *Ion Beam Therapy Fundamentals, Technology, Clinical Applications*. Springer Berlin Heidelberg; 2012:149-177. [https://doi.org/10.1007/978-3-642-21414-1\\_10](https://doi.org/10.1007/978-3-642-21414-1_10).
91. Fleury E, Trnková P, Spruijt K, et al. Characterization of the HollandPTC proton therapy beamline dedicated to uveal melanoma treatment and an interinstitutional comparison. *Med Phys* 2021;48:4506-4522. <https://doi.org/10.1002/mp.15024>.
92. Newhauser WD, Koch NC, Fontenot JD, et al. Dosimetric impact of tantalum markers used in the treatment of uveal melanoma with proton beam therapy. *Phys Med Biol* 2007;52:3979-3990. <https://doi.org/10.1088/0031-9155/52/13/021>.
93. International Atomic Energy Agency. Absorbed dose determination in external beam radiotherapy. In *Atomic Energy, Technical Reports Series No. 398*. Vienna: International Atomic Energy Agency; 2000:1-229. Accessed July 23, 2024. <https://www.iaea.org/publications/5954/absorbed-dose-determination-in-external-beam-radiotherapy>.
94. Huq MS, Fraass BA, Dunscombe PB, et al. The report of Task Group 100 of the AAPM: Application of risk analysis methods to radiation therapy quality management. *Med Phys* 2016;43:4209. <https://doi.org/10.1118/1.4947547>.
95. Arjomandy B, Taylor P, Ainsley C, et al. AAPM task group 224: Comprehensive proton therapy machine quality assurance. *Med Phys* 2019;46:e678-e705. <https://doi.org/10.1002/mp.13622>.
96. Ford E, Conroy L, Dong L, et al. Strategies for effective physics plan and chart review in radiation therapy: Report of AAPM Task Group 275. *Med Phys* 2020;47:e236-e272. <https://doi.org/10.1002/mp.14030>.
97. van Beek JGM, Ramdas WD, Angi M, et al. Local tumour control and radiation side effects for fractionated stereotactic photon beam radiotherapy compared to proton beam radiotherapy in uveal melanoma. *Radiother Oncol* 2021;157:219-224. <https://doi.org/10.1016/j.radonc.2021.01.030>.
98. Groenewald C, Konstantinidis L, Damato B. Effects of radiotherapy on uveal melanomas and adjacent tissues. *Eye (Lond)* 2013;27:163-171. <https://doi.org/10.1038/eye.2012.249>.
99. Mahdjoubi A, Najean M, Lemaitre S, et al. Intravitreal bevacizumab for neovascular glaucoma in uveal melanoma treated by proton beam therapy. *Graefes Arch Clin Exp Ophthalmol* 2018;256:411-420. <https://doi.org/10.1007/s00417-017-3834-3>.
100. Seibel I, Cordini D, Hager A, et al. Predictive risk factors for radiation retinopathy and optic neuropathy after proton beam therapy for uveal melanoma. *Graefes Arch Clin Exp Ophthalmol* 2016;254:1787-1792. <https://doi.org/10.1007/s00417-016-3429-4>.
101. Jabbarli L, Guberina M, Biewald E, et al. Scleral necrosis after brachytherapy for uveal melanoma: Analysis of risk factors. *Clin Exp Ophthalmol* 2021;49:357-367. <https://doi.org/10.1111/ceo.13928>.
102. Jabbarli L, Biewald E, Guberina M, et al. Prognostic factors for surgical treatment of radiation-induced scleral necrosis after brachytherapy for uveal melanoma. *Eur J Ophthalmol*. e-pub ahead of print, May 2024. doi:10.1177/11206721241257979.
103. Pica A, Schweizer C, Weber DC, et al. Proton therapy for uveal melanoma in Adolescents/Young adults (AYAs) and adults: A matched cohort analysis. *Pediatr Blood Cancer* 2021;68(SUPPL 5).
104. Busch C, Löwen J, Pilger D, Seibel I, Heufelder J, Joussem AM. Quantification of radiation retinopathy after beam proton irradiation in centrally located choroidal melanoma. *Graefes Arch Clin Exp Ophthalmol* 2018;256:1599-1604. <https://doi.org/10.1007/s00417-018-4036-3>.
105. Espensen CA, Kilgaard JF, Appelt AL, et al. Dose-response and normal tissue complication probabilities after proton therapy for choroidal melanoma. *Ophthalmology* 2021;128:152-161. <https://doi.org/10.1016/j.ophtha.2020.06.030>.
106. Mishra KK, Daftari IK, Weinberg V, et al. Risk factors for neovascular glaucoma after proton beam therapy of uveal melanoma: A detailed analysis of tumor and dose-volume parameters. *Int J Radiat Oncol Biol Phys* 2013;87:330-336. <https://doi.org/10.1016/j.ijrobp.2013.05.051>.
107. Romano MR, Catania F, Confalonieri F, et al. Vitreoretinal surgery in the prevention and treatment of toxic tumour syndrome in uveal melanoma: A systematic review. *Int J Mol Sci* 2021;22:10066. <https://doi.org/10.3390/ijms221810066>.
108. Yu CW, Joarder I, Micieli JA. Treatment and prophylaxis of radiation optic neuropathy: A systematic review and meta-analysis. *Eur J Ophthalmol* 2022;32:3129-3141. <https://doi.org/10.1177/11206721211067331>.
109. Marin L, Toumi E, Caujolle JP, et al. OCT-angiography for the diagnosis of radiation maculopathy in patients treated with proton beam therapy: A 2-year prospective study. *Eur J Ophthalmol* 2022;32:3035-3042. <https://doi.org/10.1177/11206721211067331>.
110. Wang Z, Nabhan M, Schild SE, et al. Charged particle radiation therapy for uveal melanoma: A systematic review and meta-analysis. *Int J Radiat Oncol Biol Phys* 2013;86:18-26. <https://doi.org/10.1016/j.ijrobp.2012.08.026>.
111. Char DH, Kroll S, Phillips TL, Quivey JM. Late radiation failures after iodine 125 brachytherapy for uveal melanoma compared with charged-particle (proton or helium ion) therapy. *Ophthalmology* 2002;109:1850-1854. [https://doi.org/10.1016/s0161-6420\(02\)01174-0](https://doi.org/10.1016/s0161-6420(02)01174-0).
112. National Comprehensive Cancer Network. Uveal melanoma. Version 1.2023. 2023. Accessed May 8, 2024. [https://www.nccn.org/professionals/physician\\_gls/pdf/uveal.pdf](https://www.nccn.org/professionals/physician_gls/pdf/uveal.pdf).
113. Sikuaide MJ, Salvi S, Rundle PA, Errington DG, Kacperek A, Rennie IG. Outcomes of treatment with stereotactic radiosurgery or proton beam therapy for choroidal melanoma. *Eye (Lond)* 2015;29:1194-1198. <https://doi.org/10.1038/eye.2015.109>.
114. Moriarty JP, Borah BJ, Foote RL, Pulido JS, Shah ND. Cost-effectiveness of proton beam therapy for intraocular melanoma. *PLoS One* 2015;10:e0127814. <https://doi.org/10.1371/journal.pone.0127814>.
115. Zytkovicz A, Daftari I, Phillips TL, Chuang CF, Verhey L, Petti PL. Peripheral dose in ocular treatments with CyberKnife and Gamma

- Knife radiosurgery compared to proton radiotherapy. *Phys Med Biol* 2007;52:5957-5971. <https://doi.org/10.1088/0031-9155/52/19/016>.
116. Liegl R, Schmelter V, Fuerweger C, et al. Robotic CyberKnife radiosurgery for the treatment of choroidal and ciliary body melanoma. *Am J Ophthalmol* 2023;250:177-185. <https://doi.org/10.1016/j.ajo.2022.12.021>.
117. Yazici G, Kiratli H, Ozyigit G, et al. Stereotactic radiosurgery and fractionated stereotactic radiation therapy for the treatment of uveal melanoma. *Int J Radiat Oncol Biol Phys* 2017;98:152-158. <https://doi.org/10.1016/j.ijrobp.2017.02.017>.
118. Dunavoelgyi R, Dieckmann K, Gleiss A, et al. Local tumor control, visual acuity, and survival after hypofractionated stereotactic photon radiotherapy of choroidal melanoma in 212 patients treated between 1997 and 2007. *Int J Radiat Oncol Biol Phys* 2011;81:199-205. <https://doi.org/10.1016/j.ijrobp.2010.04.035>.
119. Konstantinidis L, Groenewald C, Coupland SE, Damato B. Trans-scleral local resection of toxic choroidal melanoma after proton beam radiotherapy. *Br J Ophthalmol* 2014;98:775-779. <https://doi.org/10.1136/bjophthalmol-2013-304501>.